The Journal of CPRI,
Vol. 11, No. 1, March 2015 pp. 59-70

Stability analysis of multi machine system using FACTS and renewable energy source

Ravi Babu G* and Gowri Manohar T**

In this paper, to achieve damping improvement of an offshore wind farm (OWF) fed to a multi-machine system using a static synchronous compensator (STATCOM) is presented. The operating performance of the studied OWF is simulated by an equivalent aggregated doubly-fed induction generator (DFIG) driven by an equivalent aggregated wind turbine (WT) through an equivalent gearbox. A fuzzy logic controller (FLC) plus adaptive neuro-fuzzy inference system (ANFIS) are designed to achieve adequate damping characteristics to the dominant modes of the test system under various operating conditions. A frequency-domain approach based on a linearized system model using root-loci technique and a time-domain scheme based on a nonlinear system model subject to a three-phase short-circuit fault at the connected bus are systematically performed to examine the effectiveness of the proposed control schemes. It can be concluded from the simulated results that the proposed STATCOM integrated with the FLC plus ANFIS is shown to be superior for improving the stability of the system considered.

Keywords: *Doubly-fed induction generator, fuzzy logic controller, multi-machine system, offshore wind farm, stability, static synchronous compensator ANFIS.*

1.0 INTRODUCTION

Doubly-fed induction generator (DFIG) is, currently, the most employed wind generator due to its several merits. One of the advantages is the higher efficiency compared to a direct-drive wind power generation system with full-scale power converters since only about 20% of power flowing through power converter and the rest through stator without power electronics. Another advantage of a wind DFIG is the capability of decoupling control of active power and reactive power for better grid integration[1]. The operating point of the power system changes from time to time when the wind power is integrated with the power system. DFIG-based OWF connected to a power grid through a line-commutated high-voltage direct-current (HVDC) with a damping controller located at the rectifier current regulator of the HVDC link was proposed to contribute adequate damping to the OWF under various wind speeds and different disturbance conditions. But this control scheme was only suitable for the systems having a long distance from OWFs to onshore grids. In [4], a variable frequency transformer (VFT) was proposed to smooth the fluctuating active power generated by the OWF sent to the power grid and improve the damping of the OWF. These papers, however, just considered a power grid as an infinite bus that is not a practical power system.

To study the performance of a practical power system, a multi-machine power system is generally employed to replace the single-machine infinite-bus (SMIB) equivalent model.

*Assistant Professor (S.L), Dept. of EEE, Yogananda Institute of Technology & Science ,Tirupati. Andhra Pradesh - 517 501.
Mobile: 09985703878, E-mail: ravi.gotti239@gmail.com
** AssociateProfessor , Dept. of EEE,S.V.University college of Engineering,Tirupati. Andhra Pradesh - 517501.
Mobile: 09440474441, E-mail: gowrimanohart@gmail.com

In [5], The dynamic performance of DFIG-based wind turbines connected to multi-machine systems under three different configurations was presented in [6]. While a small series dynamic braking resistor was located at the stator circuit of the DFIG along with a DC-chopper braking resistor. Especially, increase of wind-power penetration could lead to the problem of sudden disconnection of considerable amount of power generation in case of a transient fault occurred in the system, causing the system to be unstable from an otherwise harmless fault condition. In this case, a static synchronous compensator (STATCOM) is the alternative for dynamic compensation of reactive power when the voltage is lower than the normal voltage range. A STATCOM can generate more reactive power than other FACTS devices like static VAR compensator (SVC). This is due to the fact that the maximum capacitive power generated by a STATCOM decreases only linearly with the bus voltage but it drops off as square of the bus voltage for an SVC. In addition, the STATCOM normally exhibits a faster response as it has no significant time delay associated with thyristor firing (in the order of 4 ms for an SVC) [8]. In [9], a STATCOM was connected at the point of common coupling (PCC) to maintain stable voltage and to improve the power quality by protecting DFIG-based wind farm connected to a weak grid from going offline during and after disturbances. In [11], performance of a permanent-magnet generator (PMG) based wind energy system employing a dynamic voltage regulator (DVR) was compared to one of the system employing a STATCOM. It is recommended to use a STATCOM in systems with large loads where reactive power consumption from the grid could cause serious effects on connected loads. Also in [12], a STATCOM with a fuzzy logic controller (FLC) was used to enhance power stability of a two-area four-generator interconnected power system. Co-operating a PI controller and an FLC applied to improve dynamic and steady-state performance of a speed controller based interior permanent-magnet synchronous motor was proposed in [13]. Simulation and experimental results were demonstrated that the superior performance of the proposed ANFIS control over conventional fixed-gain PI controller and fuzzy control. The tuning of the scaling factors of ANFIS controller with other fuzzy systems used in the excitation control of a synchronous power generator connected to an infinite bus through a transmission line was proposed in [14]. It was found that ANFIS and fuzzy controller combinations can produce a better quality control. For the purpose of improving the damping of the studied power system for grid integration of an OWF, this paper proposes a STATCOM connected to the interconnected bus of a DFIG-based OWF fed to a three-machine nine-bus system for compensating reactive power and maintaining the voltage at the connected bus. The main contribution of this study is the FLC plus ANFIS considered as a new damping controller.

In this paper a novel technique for real-time tuning of the parameters of the dual input power system stabilizers in a multi-machine system using neuro-fuzzy system, is presented. A systematic approach for generating training patterns and training of the neuro-fuzzy system is presented.

Investigations reveal that the performance of neuro-fuzzy dual input power system stabilizers in a multi-machine system is quite robust under wide variations in loading conditions

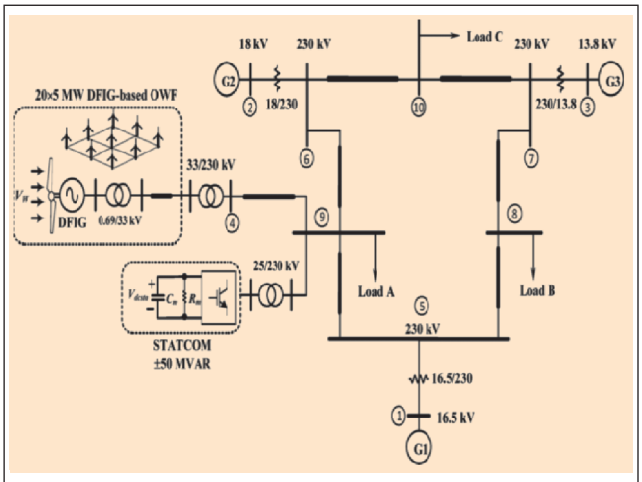

FIG. 1 CONFIGURATION OF THE SYSTEM CONSIDERED

This paper investigates the robustness of an adaptive neuro-fuzzy power system stabilizer (ANFIS PSS) [17] using the speed/acceleration state of the study unit. The proposed stabilizer is composed of a fuzzy controller transformer and an adaptive neural network. Speed deviation,

rotor angle and electrical power are chosen as the input signals to the neuro-fuzzy controller. The measured signals are the real power output and/or the speed of the study unit. From the measurements, the speed / acceleration state of the study unit is introduced, and a desired stabilizing signal is derived from the state according to pre-specified fuzzy logic control rules. The ANFIS generates supplementary control signals to conventional controllers and works adaptively in response to changes in operating conditions and network configuration. The supplementary stabilizing signals to the primary controller are utilized to improve damping of the electromechanical oscillations and to control the excitation. The control rules are quite simple so as to avoid a heavy computational burden. This is essential when considering the real time control of the study unit.

Nonlinear simulations show the robustness of the proposed ANFIS PSS subject to a wide range of loading conditions. A three-machine nine bus system is used as a model multi machine system. Comparison studies are also made between the ANFIS PSS and the FLC installed at the all subarea. The results indicate the advantages and the efficiency of the ANFIS PSS as applied to a multi machine system.

2.0 SYSTEM CONFIGURATION AND MATHEMATICAL MODELS

Figure 1 shows the configuration of the system considered. A DFIG- based OWF of 100 MW and a STATCOM of 50-MVAR are connected to bus 9 of a three-machine nine-bus system. The OWF is represented by a large equivalent aggregated DFIG driven by an equivalent aggregated variable-speed wind turbine (VSWT) through an equivalent gearbox. The employed mathematical models of the system considered are described as below.

2.1 Wind Turbine

The captured mechanical power (in W) by aVSWT can be written by

$$P = \frac{1}{2}\rho \cdot A \cdot V_{\omega}^{3} \cdot C_{p} \quad \text{....(1)}$$

Where ρ is the air density (kg/m^2), A is the blade impact area (m^2), V_W is the wind speed (m/s), and C_P is the dimensionless power coefficient of the VSWT. The power coefficient of the VSWT C_P[22] is given by

$$C_P = 0.5[(116/\lambda_i) - 0.4\cdot\beta - 5]e^{-21/\lambda_i} + 0.0068\cdot\lambda \quad \text{....(2)}$$

λTip Speed ratio (Keep the TSR constant at the optimal level at all times) [7], β Pitch angle of the blade

$$\lambda = \frac{WR}{V\omega} \quad \text{....(3)}$$

Where W Rotor angular speed in rad/sec, R Rotor blade radius in meter [22]

$$\frac{1}{\lambda_i} = \frac{1}{\lambda + 0.088\beta} + \frac{0.035}{\beta^3 + 1} \quad \text{....(4)}$$

Pitch Angle controller will start when the wind speed reaches to its rated or above rated value. Up to cut in to rated speed will maintain zero for Optimum power extraction from the wind [5]. The cut-in, rated, and cut-out wind speeds of the studied VSWT are 4, 14, and 24 m/s, respectively. When $V_W > 14$ m/s, $\beta = 0^0$. When $V_W > 14$ m/s, the pitch-angle control system activates to increase β. The two-inertia reduced-order equivalent mass-spring damper model of the VSWT coupled to the rotor shaft of the wind DFIG through an equivalent gearbox isused. The per-unit (pu) equations of motion can be referred to [2], [15], and [17].

2.2 DFIG-Based OWF Model

The stator windings of the studied wind DFIG are directly connected to the low-voltage side of the 0.69/33-kV step-up transformer while the rotor windings of the DFIG are connected to the same 0.69-kV side through a rotor-side converter (RSC), a DC link, a grid-side converter (GSC), and a connection line. For normal operation of a DFIG, the input AC-side voltages of the RSC and

the GSC can be effectively controlled to achieve the aims of simultaneous output active-power and reactive-power control [15].

Figure 2 shows the control block diagram [7] of the RSC, and the operation of the RSC requires i_{qrw} and i_{drw} to follow the varying reference points that are determined by maintaining the output active power and the stator-winding voltage at the setting values, respectively. The required voltage for the RSC (v_{rw}) is derived by controlling the pu d- and q-axis currents of the RSC. The control block diagram [7] of the GSC is shown in Figure 3. The pu d- and q-axis currents of the GSC, i_{qgw} and i_{dgw} , have to track the reference points that are determined by maintaining the DC link voltage V_{dcw} at the setting value and keeping the output of the GSC (V_{gw}) at unity power factor, respectively. The required pu voltage of the GSC is derived by controlling the per-unit d- and q-axis currents of the GSC [2].

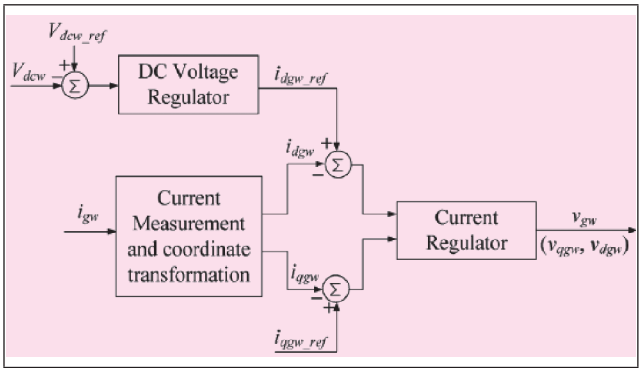

FIG. 2 CONTROL BLOCK DIAGRAM FOR THE GSC OF THE STUDIED WIND DFIG

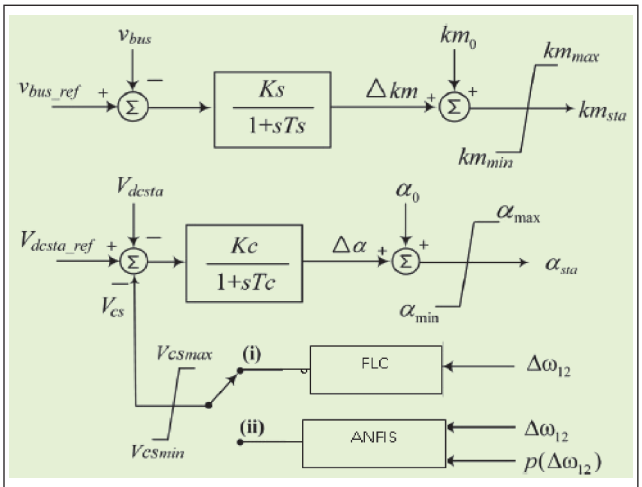

FIG. 3 CONTROL BLOCK DIAGRAM OF THE EMPLOYED STATCOM INCLUDING THE DESIGNED PID HYBRID PID PLUS FLC DAMPING CONTROLLERS

2.3 STATCOM MODEL

The pu d- and q-axis output voltages [20] of the STATCOM shown in Figure 1 can be written by, respectively,

$$v_{dsta} = V_{dcsta} \cdot Km_{sta} \cdot \sin(\theta_{bus} + \alpha_{sta}) \quad ....(5)$$

$$v_{qsta} = V_{dcsta} \cdot Km_{sta} \cdot \cos(\theta_{bus} + \alpha_{sta}) \quad ....(6)$$

where v_{dsta} and v_{dsta} are the pu d- and q-axis voltages at the output terminals of the STATCOM, respectively; Km_{sta} and α_{sta} are, respectively, the modulation index and phase angle of the STATCOM; θ_{bus} is the voltage phase angle of the common AC bus, and V_{dcsta} is the pu DC voltage of the DC capacitor C_m. The pu DC voltage-current equation of the DC capacitor C_m can be described by

$$(C_m)\, p\, (V_{dcsta}) = W_b\, [I_{dcsta} - (\frac{V_{dcsta}}{R_m})] \quad ....(7)$$

where p is a differential operator with respect to time t and

$$I_{dcsta} = i_{dsta} \cdot Km_{sta} \cdot \sin(\theta_{bus} + \alpha_{sta}) + i_{qsta} \cdot Km_{sta} \cdot \cos(\theta_{bus} + \alpha_{sta}) \quad ....(8)$$

is the pu DC current flowing into the positive terminal of V_{dcsta}, R_m is the pu equivalent resistance considering the equivalent electrical losses of the STATCOM, and i_{dsta} and i_{qsta} are the pu d- and q-axis currents flowing into the terminals of the STATCOM, respectively. The pu DC voltage is V_{dcsta} controlled by α_{sta} while the AC voltage V_{sta} is varied by changing Km_{sta} .

2.4 Three-Machine Nine-Bus System

The well-known three-machine nine-bus power system which is widely used in power system stability studies was shown in Figure 1. The complete parameters of this system can be referred to [20]. In this paper, each synchronous generator is represented by a two-axis model whose block diagram is shown in Figure 4. In this model, the transient effects are accounted for

while the sub transient effects are neglected. The additional assumptions made in this model are that the transformer-voltage terms in the stator voltage equations are negligible compared to the speed-voltage terms and the rotational speed is approximate to the rated speed of 1.0 pu. The pu differential equations for the *i*-th synchronous generator are described as follows:

$$(T'_{qoi})\, p\,(E'_{di}) = -E'_{di} - (X_{qi} - X'_{qi})\, I_{qi} \quad ....(9)$$

$$(T'_{doi})\, p\,(E'_{qi}) = -E'_{qi} + E_{FDi} + (X_{di} - X'_{di})\, I_{di} \quad ....(10)$$

$$(T_{ji})\, p\,(w_i) = T_{Mi} - [\, I_{di}\, E'_{di} + I_{qi}\, E'_{qi} - (L'_{qi} - L'_{di})\, I_{di}\, I_{di}] - p_i w_i \quad ....(11)$$

$$P(\delta_i) = w_i - 1. \quad ....(12)$$

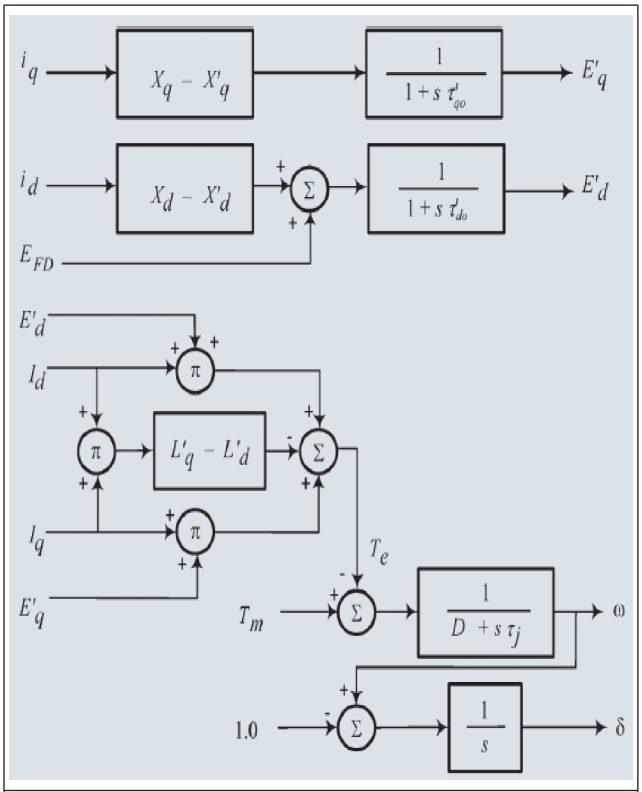

FIG. 4 BLOCK DIAGRAM REPRESENTATION OF TWO-AXIS MODEL FOR THE STUDIED SYNCHRONOUS GENERATOR.

Consider the multi-machine system with constant impedance loads shown in Figure 5 whose network has three generators and three loads.

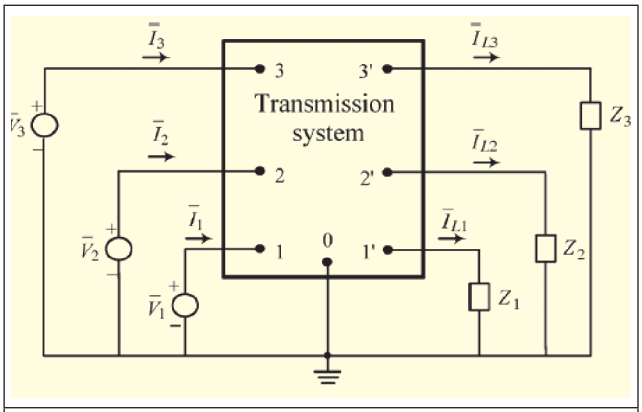

FIG. 5 MULTI-MACHINE SYSTEM WITH CONSTANT IMPEDANCE LOADS

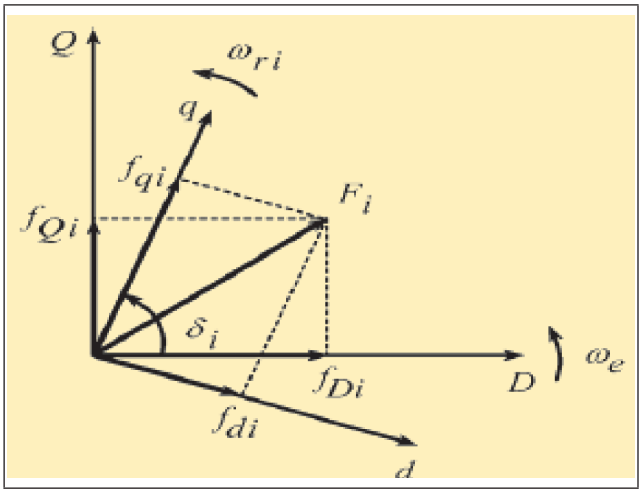

FIG. 6 TRANSFORMATION FROM THE TH SYNCHRONOUS GENERATOR'S ROTOR REFERENCE FRAME TO THE COMMON DQ REFERENCE FRAME

Assume that the three loads are represented by three constant impedances while three generators are represented by three active sources. Therefore, all the nodes have zero injection currents except for the generator nodes. This property is used to obtain the network reduction as shown below. With the relation between nodal currents and voltages is

$$I = \overline{Y}_{sys}\, V \quad ....(13)$$

$$\begin{bmatrix} I_3 \\ 0 \end{bmatrix} = \begin{bmatrix} y_{31} & y_{32} \\ y_{33} & y_{34} \end{bmatrix} \begin{bmatrix} V_{31} \\ V_{32} \end{bmatrix} \quad ....(14)$$

Where $I_3 = [\bar{I}_{L1}\ \bar{I}_{L2}\ \bar{I}_{L3}]^T$ is the injected current vector at generator nodes, $V_{31} = [\bar{V}_1\ \bar{V}_2\ \bar{V}_3]^T$ is the voltage vector at the generator nodes, $V_{32} = [\bar{V}_{1'}\ \bar{V}_{2'}\ \bar{V}_{3'}]^T$ is the voltage vector at the eliminated

nodes, and y_{sys} is the original system admittance matrix. Expanding the above equations, it yields

$$I_3 = Y_{31} V_{31} + Y_{32} V_{32} \text{ and}$$
$$0 = Y_{33} V_{31} + Y_{34} V_{32} \quad ....(15)$$

From (15), V_{32} can be eliminated to get

$$I_3 = (Y_{31} - Y_{32} Y^{-1}_{34} Y_{33}) V_{31} \quad ....(16)$$

$$\overline{Y} = (Y_{31} - Y_{32} Y^{-1}_{34} Y_{33}) \quad ....(17)$$

where $\overline{Y}$ is the desired reduced admittance matrix and it has the dimensions of 3X̊3. Since each generator is modeled under its own dq-axis reference frame rotating with its rotor, the transformation from each synchronous generator's dq-axis rotor reference frame to the common DQ-axis reference frame is shown in Figure 6 and can be given as follows:

$$\begin{bmatrix} f_D \\ f_Q \end{bmatrix} = \begin{bmatrix} sin\delta_i & -cos\delta_i \\ cos\delta_i & sin\delta_i \end{bmatrix} \begin{bmatrix} f_{di} \\ f_{qi} \end{bmatrix} \quad ....(18)$$

where*f* can be either a current *i* or a voltage v while δ*i* is the angle between the q-axis of the *i*-th synchronous generator and the common *Q*-axis.

3. DESIGN OF DAMPING CONTROLLERS FOR STATCOM

3.1 Design of an FLC

This section employs the technique of FLC theorem to design the FLC controller, the following fundamental design steps for a FLC are employed and referred to [17] including: 1) fuzzification (FI), 2) decision-making logic (DML), 3) defuzzification (DFI), and 4) knowledge base (KB). This paper utilizes the Sugeno-type fuzzy inference system since it works well with linear, optimization, and adaptive techniques. Seven linguistic variables for each input variable are used. These are NB (Negative Big), NM (Negative Medium), NS (Negative Small), ZR (Zero), PS (Positive Small), PM (Positive Medium), and PB (Positive Big). There are also seven linguistic variables for output variable, namely, IB (Increase Big), IM (Increase Medium), IS (Increase Small), KV (Keep Value), DS (Decrease Small), DM (Decrease Medium), and DB (Decrease Big). The control rules subject to the two input signals and the output signal are listed in Table 1 [7].

3.2 Adaptive Neuro-Fuzzy Method

Adaptive neuro-fuzzy method (or Adaptive neuro-fuzzy inference system, ANFIS) has been

TABLE 1
CONTROL RULES OF THE STUDIED FUZZY LOGIC CONTROLLER

	NB	**NM**	**NS**	**ZR**	**PS**	**PM**	**PB**
PB	KV	IS	IM	IB	IB	IB	IB
PM	DS	KV	IS	IM	IB	IB	IB
PS	DM	DS	KV	IS	IM	IB	IB
ZR	DB	DM	DS	KV	IS	IM	IB
NS	DB	DB	DM	DS	KV	IS	IM
NM	DB	DB	DB	DM	DS	KV	IS
NB	DB	DB	DB	DB	DM	DS	KV

became a popular method in control area. In this section, we give a brief description of the principles of Adaptive neuro-fuzzy inference system (ANFIS) which are referred to [18] and [19]. The basic structure of the type of fuzzy inference system could be seen as a model that maps input characteristics to input membership functions. Then it maps input membership function to rules and rules to a set of output characteristics. Finally it maps output characteristics to output membership functions, and the output membership function to a single valued output or a decision associated with the output. It has been considered only fixed membership functions that were chosen arbitrarily. Fuzzy inference is only applied to only modeling systems whose rule structure is essentially predetermined by the user's interpretation of the characteristics of the variables in the model. However, in some modeling situations, it cannot be distinguish what the membership functions should look like simply from looking at data. Rather than choosing the parameters associated with a given

membership function arbitrarily, these parameters could be chosen so as to tailor the membership functions to the input/output data in order to account for these types of variations in the data values. In such case the necessity of the adaptive neuro fuzzy inference system becomes obvious. Neuro-adaptive learning techniques provide a method for the fuzzy modeling procedure to learn information about a data set. It computes the membership function parameters that best allow the associated fuzzy inference system to track the given input/output data. A network-type structure similar to that of a neural network can be used to interpret the input/output map so it maps inputs through input membership functions and associated parameters, and then through output membership functions and associated parameters to outputs,. The parameters associated with the membership functions changes through the learning process. The computation of these parameters (or their adjustment) is facilitated by a gradient vector. This gradient vector provides a measure of how well the fuzzy inference system is modeling the input/output data for a given set of parameters. When the gradient vector is obtained, any of several optimization routines can be applied in order to adjust the parameters to reduce some error measure (performance index). This error measure is usually defined by the sum of the squared difference between actual and desired outputs. ANFIS uses a combination of least squares estimation and back propagation for membership function parameter estimation.

The suggested ANFIS has several properties:

- The output is zeroth order Sugeno-type system.
- It has a single output, obtained using weighted average defuzzification. All output membership functions are constant.
- It has no rule sharing. Different rules do not share the same output membership function, namely the number of output membership functions must be equal to the number of rules.
- It has unity weight for each rule.

Figure 7 shows Sugeno's fuzzy logic model. Figure 8 shows the architecture of the ANFIS, comprising by input, fuzzification, inference and defuzzification layers. The network can be visualized as consisting of inputs, with N neurons in the input layer and F input membership functions for each input, with F*N neurons in the fuzzification layer. There are F^N rules with F^N neurons in the inference and defuzzification layers and one neuron in the output layer. For simplicity, it is assumed that the fuzzy inference system under consideration has two inputs x and y and one output z as shown in Figure 8. For a zero-order Sugeno fuzzy model, a common rule set with two fuzzy if-then rules is the following:

Rule 1: If x is A1 and y is B1, Then f1 = r1

Rule 2: If x is A2 and y is B2, Then f2 = r2

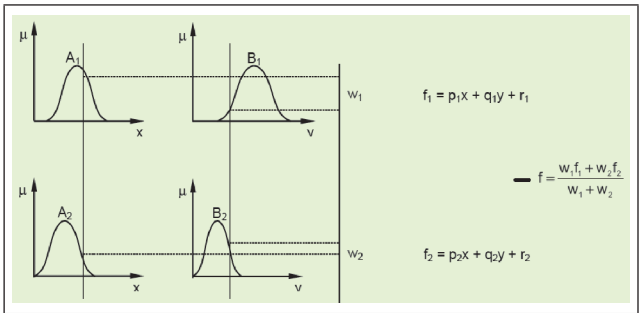

FIG. 7 SUGENO'S FUZZY LOGIC MODEL

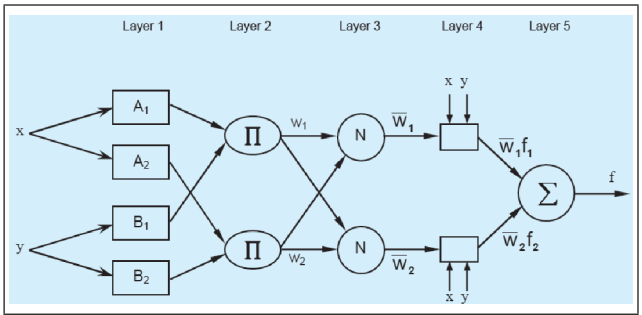

FIG. 8 THE ARCHITECTURE OF ANFIS

4.0 METHODOLOGY

The procedure of this research is shown in Figure 9. The simulation environment based on MATLAB™ software package is selected. It is used as the main engineering tool for performing modeling and simulation of multi-machine power systems, as well as for interfacing the user and

appropriate simulation programs. MATLAB™ has been chosen due to availability of the powerful set of programming tools, signal processing, numerical functions, and convenient user-friendly interface. In this specially developed simulation environment, the evaluation procedures can be easily performed. We have used Fuzzy logic Toolbox of MATLAB™ to develop the ANFIS model with 4 inputs and single output as given in Figure 8.

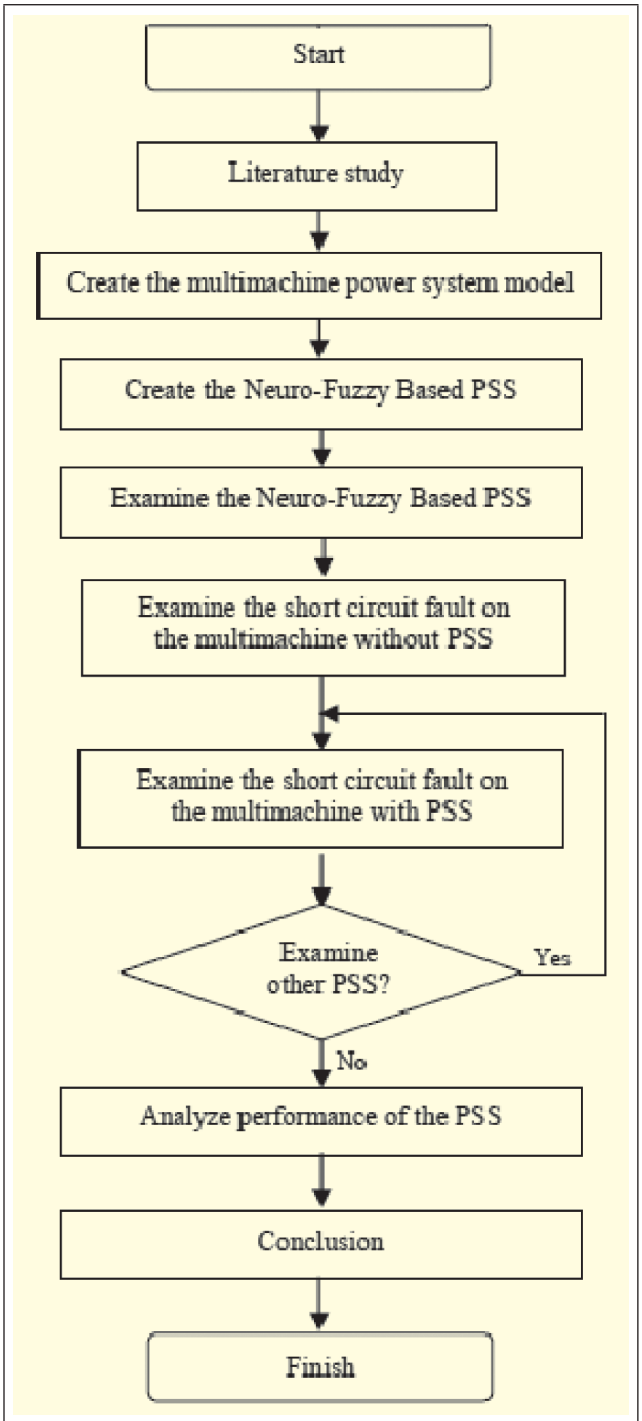

FIG. 9 FLOW CHART OF THE PROPOSED METHOD.

5.0 SIMULATION RESULTS

This section uses the nonlinear system model developed to compare the damping characteristics contributed by the proposed STATCOM joined with the designed FLC controller and FLC plus ANFIS controller on stability improvement of the system considered under a three-phase short-circuit fault at bus 9 of Figure 1. The three-phase short-circuit fault is suddenly applied to bus 9 at t=1s and is cleared at t=1.1s. Although this type of fault seldom occurs in practical power systems, it is the most critical and the most severe fault to check whether the system considered can withstand such severe system impacts. If the system considered are stable when this severe fault is suddenly applied and is cleared by some protective relays, it means that the system considered have ability to remain stable operation when the systems are subject to other faults such as single line-to-ground fault, line-to-line fault, etc. It is assumed that the DFIG-based OWF operates under a base wind speed of 12 m/s while the three-machine system operates under a stable condition. The simulation results of the proposed system using MATLAB™/ SIMULINK toolbox are presented in Figure 10. This figure plots the comparative transient responses of the system considered with the proposed STATCOM without controller, with the designed FLC controller and with the FLC plus ANFIS controller. It is clearly observed from the comparative transient simulation results shown in Figure 10 that the proposed STATCOM with the designed FLC plus ANFIS controller can offer better damping characteristics than the designed FLC controller.

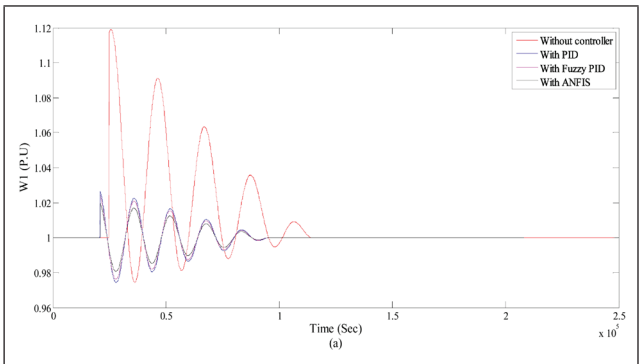

FIG. 10 (A) ROTOR SPEED OF G1

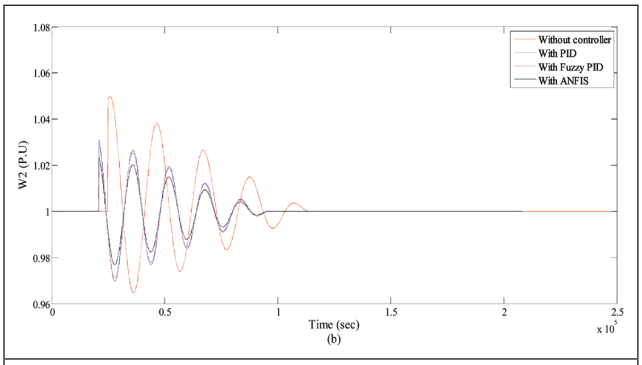

FIG. 10 (B) ROTOR SPEED OF G2

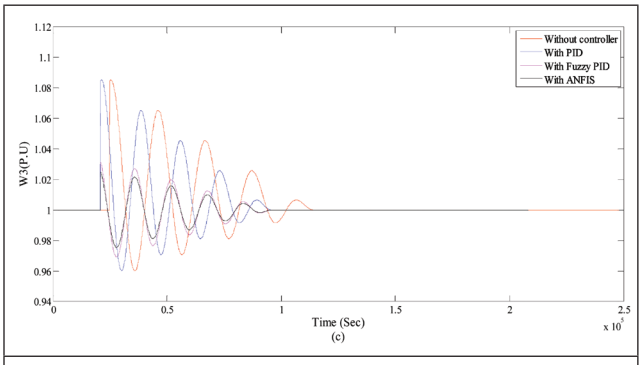

FIG. 10 (C) ROTOR SPEED OF G3

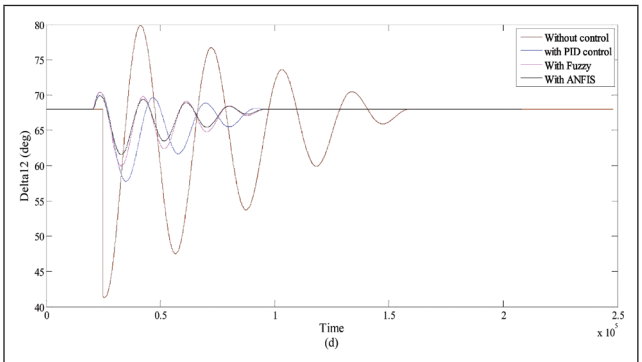

FIG. 10 (D) ROTOR ANGLE DEVIATION BETWEEN G1 TO G2

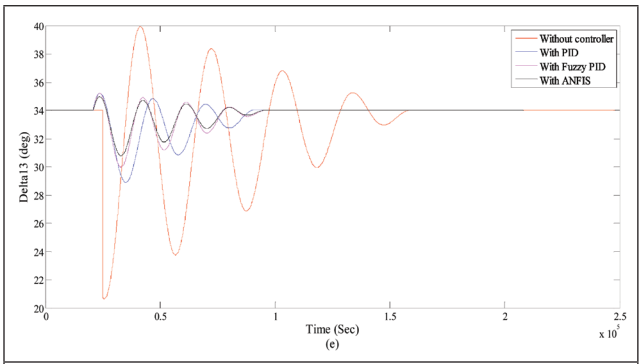

FIG. 10 (E) ROTOR ANGLE DEVIATION BETWEEN G1 TO G3

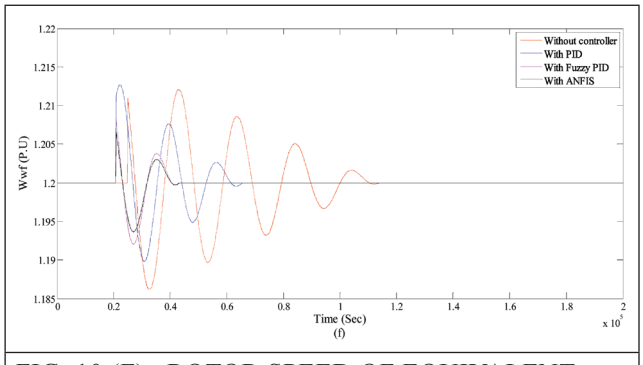

FIG. 10 (F) ROTOR SPEED OF EQUIVALENT DFIG-BASED OWF

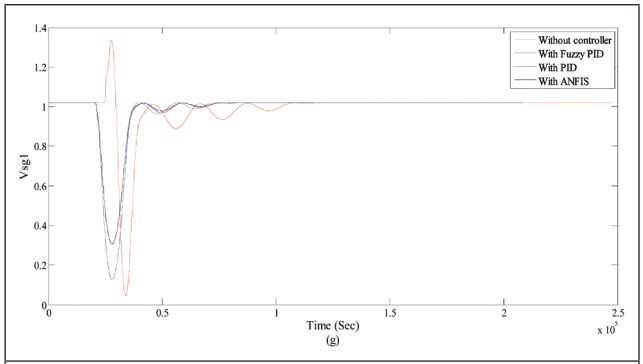

FIG. 10 (G) TERMINAL VOLTAGE OF G1

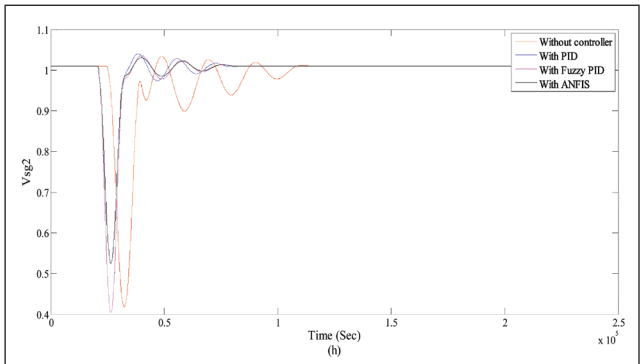

FIG. 10 (H) TERMINAL VOLTAGE OF G2

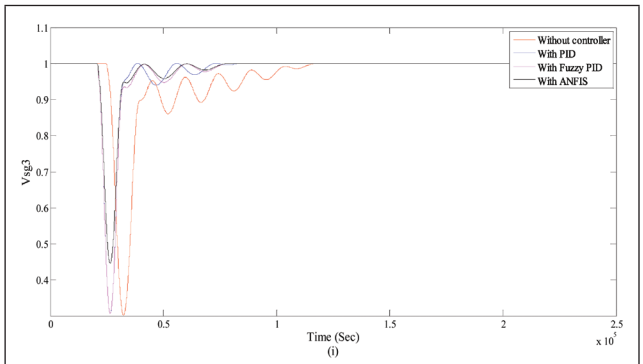

FIG. 10 (I) TERMINAL VOLTAGE OF G3

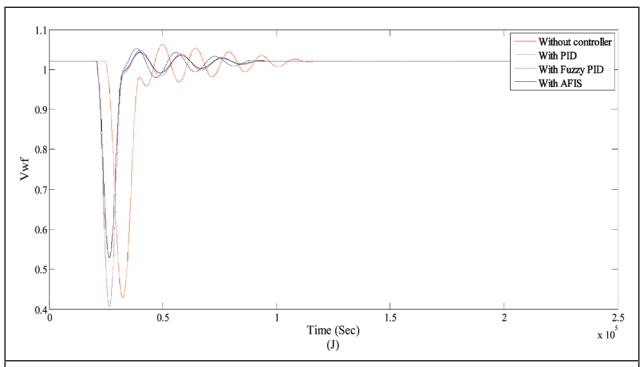

FIG. 10 (J) VOLTAGE OF OWF

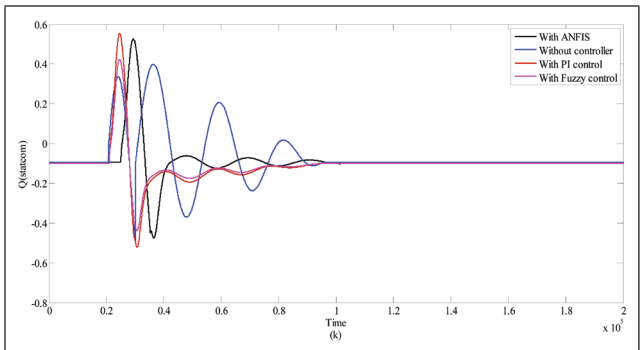

FIG. 10 (K) REACTIVE POWER SUPPLIED BY STATCOM.

REFERENCES

[1] R Pena, J C Clare and G M Asher, "Doubly fed induction generator using back-to-back PWM converters and its application to variable speed wind-energy generation," *Proc. Inst. Elect. Eng., Elect. Power Appl.*, vol. 143, no. 3, pp. 231–241, May 1996.

[2] L Wang and K -HWang, "Dynamic stability analysis of a DFIG-based offshore wind farm connected to a power grid through an HVDC link," *IEEE Trans. Power Syst.*, vol. 26, no. 3, pp. 1501–1510, Aug. 2010.

[3] L Wang and L -Y Chen, "Reduction of power fluctuations of a largescale grid-connected offshore wind farm using a variable frequency transformer," *IEEE Trans. Sustain. Energy*, vol. 2, no. 3, pp. 226–234, Apr. 2011.

[4] E Muljadi, T B Nguyen, and M A Pai, "Impact of wind power plants on voltage and transient stability of power systems," in *Proc. IEEE Energy 2030 Conf.*, Nov. 2008, pp. 1–7.

[5] O Anaya-Lara, A Arulampalam, G. Bathurst, F. M. Hughes, and N. Jenkins, "Transient analysis of DFIG wind turbines in multi-machine networks," in *Proc. 18th Int. Conf. Exhib. Electricity Distribution CIRED*, Jun. 2005, pp. 1–5.

[6] K E Okedu, S M Muyeen, R Takahashi, and J Tamura, "Improvement of fault ride through capability of wind farms using DFIG considering SDBR," in *Proc. 14th Eur. Conf. Power Electronics and Applications*, Sep. 2011, pp. 1–10.

[7] Li Wang and Dinh-Nhon Truong "Stability Enhancement of DFIG-Based offshore wind farm fed to a Multi-Machine system using a STATCOM," IEEE Transactions on Power Systems., vol. 143, no. 3, pp. 231–241, May 1996

[8] B Pokharel and W Gao, "Mitigation of disturbances in DFIG-based wind farm connected to weak distribution system using STATCOM," in *Proc. North American Power Symp. (NAPS)*, Sep. 26–28, 2010, pp. 1–7.

[9] G Cai, C Liu, Q Sun, D Yang, and P Li, "A new control strategy to improve voltage stability of the power system containing large-scale wind power plants," in *Proc. 4th Int. Conf. Electric Utility Deregulation and Restructuring and Power Technologies (DRPT)*, Jul. 2011, pp. 1276–1281.

[10] M N Eskander and S I Amer, "Mitigation of voltage dips and swells in grid-connected wind energy conversion systems," in *Proc. ICCASSICE*, Aug. 2009, pp. 885–890.

[11] L O Mak, Y X Ni, and C M Shen, "STATCOM with fuzzy controllers for interconnected power systems," *Elect. Power Syst. Res.*, vol. 55, no. 2, pp. 87–95, Aug. 2000.

[12] M N Uddin and R S Rebeiro, "Improved dynamic and steady state performance of a hybrid speed controller based IPMSM drive," in *Proc. IEEE Industry Applications Society Annual Meeting (IAS)*, Oct. 9–13, 2011, pp. 1–8.

[13] L Reznik, O Ghanayem and A Bourmistrov, "PID plus fuzzy controller structures as a design base for industrial applications," *Eng.Appl. Artif. Intell.*, vol. 13, no. 4, pp. 419–430, Aug. 2000.

[14] S M Muyeen, M H Ali, R Takahashi, T Murata, J Tamura, Y Tomaki, A Sakahara, and E Sasano, "Transient stability analysis of wind generator system with the consideration of multi-mass shaft model," in *Proc. Int. Conf. Power Electronics and Drives Systems*, Jan. 16–18, 2006, vol. 1, pp. 511–516.

[15] P Cartwright, L Holdsworth, J B Ekanayake, and N Jenkins, "Coordinated voltage control strategy for a doubly-fed induction generator (DFIG)-Based wind farm," *Proc. Inst. Elect. Eng., Gener. Transm.,Distrib.*, vol. 151, no. 4, pp. 495–502, Aug. 2004.

[16] L Wang and C -T Hsiung, "Dynamic stability improvement of an integrated grid-connected offshore wind farm and marine-current farm using a STATCOM," *IEEE Trans. Power Syst.*, vol. 26, no. 2, pp. 690–698, May 2011.

[17] E1shafei. AL. K E1-Metwal1y andAA Sha1tout. 2005. A variable structure adaptive fzzy logic stabilizer for single and multi-machine power systems. *Control Engineering Practice, Elsevier,* 13: 413-423.

[18] Fraile-Ardanuy, J and P J Zufiria. 2005. Adaptive Power System Stabilizer Using ANFIS and Genetic Algorithms, *Proceedings of the 44th IEEE Conference on Decision and Control, and the European Control Conference 2005 Seville, Spain, December 12-15, 2005*, pp. 8028-8033.

[19] N G Hingorani and L Gyugyi, *Understanding FACTS; Concepts and Technology of Flexible AC Transmission Systems*. NewYork,NY, USA: IEEE Press, 2000.

[20] P M Anderson and A A Fouad, *Power System Control and Stability*.Ames, IA, USA: Iowa State Univ. Press, 1977.

[21] Jyothsna T R , & Vaisakh K 2009. Multi-objective Evolutionary Programming Based Design of PSS, SVC, and TCSC for Transient Stability Improvement, Proceedings of World Academy of Science: Engineering & Technology; 39, 859-863.

[22] Wu, Y Lang, N Zargari and S Kouro" Conversion and Control Of Wind Energy Systems Wiley – IEEE Press First Edition.